

# A Silicon Resonate-and-Fire Neuron Based on the Volterra System

Kazuki Nakada<sup>†</sup>, Tetsuya Asai<sup>‡</sup>, and Hatsuo Hayashi<sup>†</sup>

<sup>†</sup>Graduate School of Life Science and Systems Engineering, Kyushu Institute of Technology  
2-4 Hibikino, Wakamatsu-ku, Kitakyushu, Fukuoka 808-0196, Japan

<sup>‡</sup>Graduate School of Information Science and Technology, Hokkaido University  
Kita 14, Nishi 9, Kita-ku, Sapporo, Hokkaido 060-0814, Japan,  
Email: nakada@brain.kyutech.ac.jp

**Abstract**—We propose an analog integrated circuit that implements a resonate-and-fire neuron (RFN) model based on the Volterra system. The RFN model is a simple spiking neuron model that exhibits dynamic behavior observed in biological neurons, such as fast subthreshold oscillation, post-inhibitory rebound, and frequency preference. The RFN circuit was derived from the Volterra system to mimic such behaviors of the RFN model. Through circuit simulations, we will show that our circuit is expected to be useful for large-scale integrated circuit implementation of functional spiking neural networks since it acts as a coincidence detector and a band-pass filter at a single unit level.

## 1. Introduction

Many recent advances in neuromorphic engineering are associated with functional silicon spiking neural networks, which consist of the electronic analogue of the integrate-and-fire neuron (IFN) model [3]-[8]. In such silicon spiking neural networks, coincidence or synchrony detection plays functional roles in neural information processing, such as auditory perception [5], onset detection [6], learning and memory [7], and image processing [8]. Temporal filtering properties are also significant to extract temporal structure of spike sequences in which information may be encoded.

Silicon spiking neural networks have computational limitations if their components are quite simple. For instance, the Axon-Hillock circuit [1], widely known as the traditional IFN circuit, can only act as a high pass-filter. Therefore, many neuromorphic engineers have developed alternative IFN circuits [9]-[15], such as a low-power adaptive IFN circuit with frequency adaptation [13]. These circuits increase the sensitivity to signal detection in silicon spiking neural networks. Short-term dynamic synapse circuits [6], [7], [17]-[19] also increase the computational power of the silicon spiking neural networks because they act as additional filters to inputs in an IFN [18]. In fact, a depressing synapse circuit enables a silicon spiking neural network to detect burst synchrony [6]. Spike-timing-dependent synaptic plasticity (STDP) circuits can also enhance synchrony detection in silicon spiking neural networks

[7], [20]. These results imply that additional circuits that have temporal filtering and synchrony detection properties work effectively to increase computational performances of silicon spiking neural networks.

In this paper, we propose an analog metal-oxide-semiconductor (CMOS) circuit of a resonate-and-fire neuron (RFN) model [21]. The RFN model is a simple spiking neuron model that exhibits dynamic behaviors observed in biological neurons, such as fast subthreshold oscillation, post-inhibitory rebound, and frequency preference. We implemented the RFN circuit based on the Volterra system [23] to mimic such behavior of the RFN model. By using the circuit simulator, HSPICE, we will show that the RFN circuit is expected to be useful for large-scale integrated circuit implementation of functional spiking neural networks since the circuit acts as a coincidence detector and a band-pass filter at a single unit level.

## 2. Resonate-and-Fire Neuron Model

The resonate-and-fire neuron (RFN) is a simple spiking neuron model proposed by Izhikevich [21]. The dynamics of the RFN model are described by:

$$\dot{x} = bx - wy + I \quad (1)$$

$$\dot{y} = wx + by \quad (2)$$

or by an equivalent complex form:

$$\dot{z} = (b + iw)z + I \quad (3)$$

where  $z = x + iy$  is a complex variable, the real and imaginary parts,  $x$  and  $y$ , are the current- and voltage-like variables, respectively,  $b$  and  $w$ , are parameters, and  $I$  is an external input.

If  $\text{Im } z$  exceeds certain threshold  $a_{\text{th}}$ ,  $z$  is reset to arbitrary value  $z_o$ , which describes an activity-dependent after-spike reset. This model has second-order membrane dynamics, and thus exhibits various dynamic behaviors, such as fast damped subthreshold oscillation, resulting in frequency preference and post-inhibitory rebound [21].

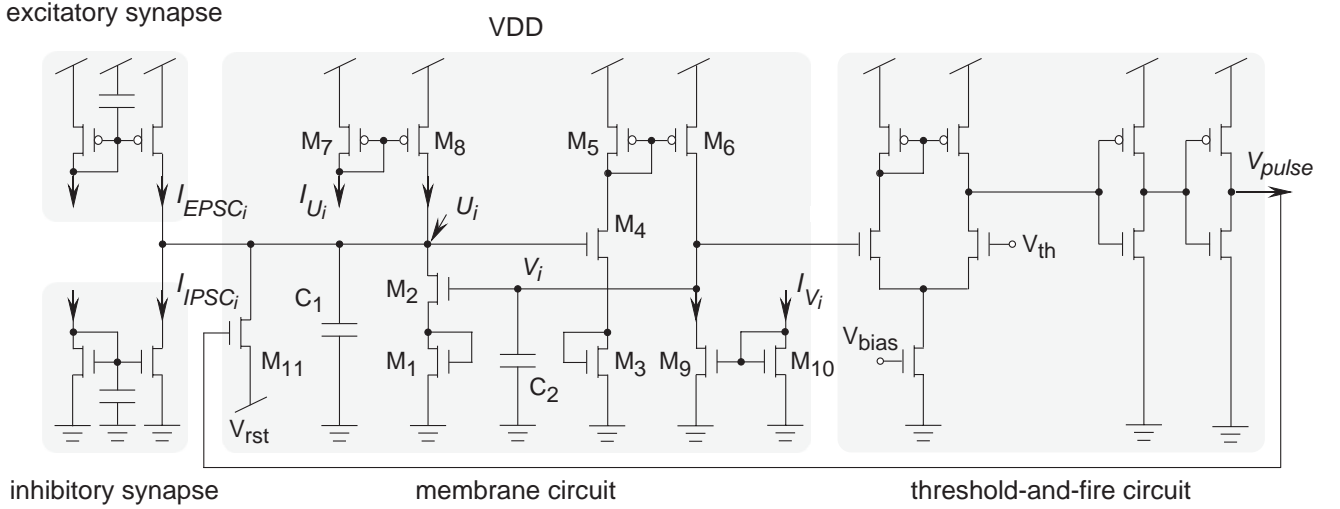


Figure 1: Schematic of the resonate-and-fire neuron circuit.

### 3. Resonate-and-Fire Neuron Circuit Based on the Volterra System

We here propose an analog integrated circuit that implements the RFN model. The RFN circuit consists of a membrane circuit, a threshold-and-fire circuit, and current mirror integrators as excitatory and inhibitory synapses [2] (Fig. 1).

The membrane circuit was derived from the Volterra system for modeling prey-predator interactions [23] to mimic membrane dynamics of the RFN model. The Volterra system is described as follows:

$$\dot{z}_1 = z_1(a - z_1) \quad (4)$$

$$\dot{z}_2 = z_2(z_2 - 1) \quad (5)$$

where  $z_1$  and  $z_2$  correspond to the prey and predator population, respectively, and  $a$  is a positive constant. By replacing  $z_i = b_i \exp x_i$  ( $i = 1, 2$ ), these equations can be rewritten as following:

$$\dot{x}_1 = a - b_1 \exp x_1 \quad (6)$$

$$\dot{x}_2 = b_2 \exp x_2 - 1 \quad (7)$$

where  $b_1$  and  $b_2$  are positive constants. Eqs. (6) and (7) can easily be implemented into silicon chips using the current-voltage relationship of subthreshold MOS FETs [14]. Saturation current  $I$  for an nMOS FET operating in the subthreshold region is described by:

$$I = I_o \exp\left(\frac{\kappa V_g - V_s}{V_T}\right) \quad (8)$$

where  $V_g$  is the gate voltage,  $V_s$  is the source voltage,  $I_o$  the pre-exponential current,  $\kappa$  the capacitive coupling ratio from the gate to the channel, and  $V_T$  the thermal voltage [2].

We designed the membrane circuit by using the above relationships (6), (7) and (8). The dynamics of the membrane circuit is described as following:

$$C_1 \frac{dU_i}{dt} = -gU_i + I_{in} + I'_{U_i} - I_o \exp\left(\frac{\kappa^2}{\kappa + 1} \frac{V_i}{V_T}\right) \quad (9)$$

$$C_2 \frac{dV_i}{dt} = I_o \exp\left(\frac{\kappa^2}{\kappa + 1} \frac{U_i}{V_T}\right) - I'_{V_i} \quad (10)$$

where  $U_i$  and  $V_i$  are voltages corresponding to state variables,  $g$  the voltage-dependent conductance of the transistor  $M_{11}$ ,  $C_1$  and  $C_2$  the capacitances, and  $I_{in}$  a summation of external currents:

$$I_{in} = I_{EPSC_i} - I_{IPSC_i} \quad (11)$$

where  $I_{EPSC_i}$  and  $I_{IPSC_i}$  are the post synaptic currents through the excitatory and inhibitory synapses. Current  $I'_{U_i}$  through  $M_8$  and the current  $I'_{V_i}$  through  $M_9$  are approximately described as following:

$$I'_{U_i} = \alpha I_{U_i} \left(1 + \frac{VDD - U_i}{V_{E,p}}\right) \quad (12)$$

$$I'_{V_i} = \beta I_{V_i} \left(1 + \frac{V_i}{V_{E,n}}\right) \quad (13)$$

where  $I_{U_i}$  and  $I_{V_i}$  are the bias currents, VDD the power-supply voltage,  $V_{E,p}$  and  $V_{E,n}$  the Early voltage [2] for nMOS and pMOS FETs, respectively, and  $\alpha$  and  $\beta$  the proportional constants. If the Early voltages of  $M_7$ ,  $M_8$ ,  $M_9$ , and  $M_{10}$  are large enough to neglect the drain-to-source voltage dependence of currents through the transistors,  $I'_{U_i}$  and  $I'_{V_i}$  are constant. Furthermore, if the leak conductance  $g$  is zero, the circuit dynamics described by (9) and (10) are equivalent to (6) and (7), respectively. In this case, the membrane circuit shows nonlinear oscillation depending on the stability of the equilibrium point of the circuit.

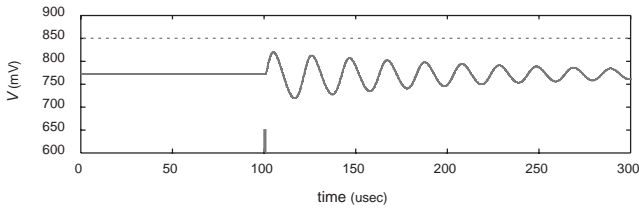


Figure 2: Subthreshold oscillation.

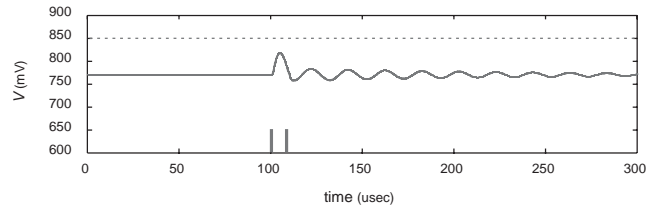


Figure 4: Non-resonant response.

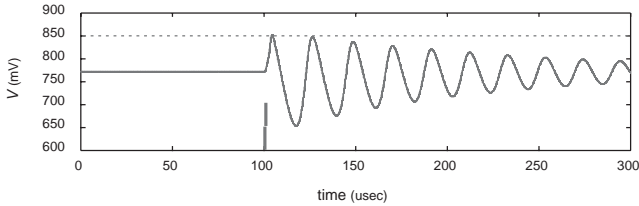


Figure 3: Coincidence detection.

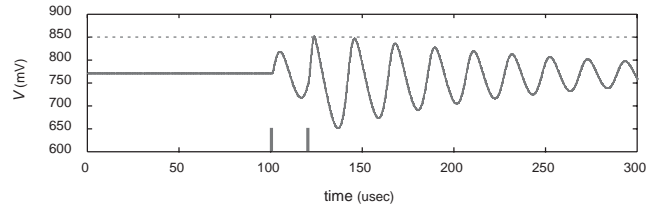


Figure 5: Resonant response.

Equilibrium point of the circuit,  $(U_o, V_o)$ , can easily be calculated, and the stability of the points can be analyzed by eigenvalues of the Jacobian matrix of the circuit,

$$J = \begin{bmatrix} -\frac{\alpha I_{U_i}}{V_{E,p}} & -\frac{\kappa}{\kappa+1} \frac{I_{V_o}}{V_T} \\ \frac{\kappa}{\kappa+1} \frac{I_{U_o}}{V_T} & -\frac{\beta I_{V_i}}{V_{E,n}} \end{bmatrix} \quad (14)$$

where  $I_{U_o}$  and  $I_{V_o}$  represent the equilibrium currents at the equilibrium point  $(U_o, V_o)$ . We used the shortest transistors that had small Early voltages for  $M_7$ - $M_{10}$  and diode-connected transistors  $M_1$ - $M_4$ . As a result, the equilibrium point became a focus, and thus the circuit exhibited fast damped oscillation in response to inputs. In this case, the circuit dynamics is equivalent to the membrane dynamics of the RFN model near the equilibrium point.

Inputs through excitatory and inhibitory synapse change the amplitude and phase of the oscillation of the membrane circuit. The threshold-and-fire circuit generates a spike (a pulse voltage  $V_{\text{pulse}}$ ) and resets  $U_i$  to voltage  $V_{\text{rst}}$  if  $V_i$  exceeds a threshold voltage  $V_{\text{th}}$ . Thus, the behavior of the RFN circuit is qualitatively the same as that of the RFN model.

#### 4. Simulation Results

We verified the desired operation of the RFN circuit using the circuit simulator, HSPICE, with the model parameters for the 0.35- $\mu\text{m}$  CMOS process.

In the following simulations, we set a parameter sets as follows:  $V_{\text{DD}}=2$  V,  $V_{\text{bias}}=1$  V,  $V_{\text{th}}=850$  mV,  $V_{\text{rst}}=720$  mV,  $I_{U_i}=I_{V_i}=10$  nA, and  $C_1=C_2=0.5$  pF. We used pulse currents (width: 1  $\mu\text{sec}$ ) as excitatory and inhibitory inputs.

Figure 2 shows a damped subthreshold oscillation in response to a weak input (amplitude: 30 nA). When two weak inputs arrive at the circuit within about 2  $\mu\text{s}$  (Fig. 3) or the interval of the two inputs is nearly equal to the period of the oscillation, 20  $\mu\text{s}$  (Fig. 5), the circuit fires a spike. However, the circuit does not fire a spike when the interval of the two inputs is in other ranges, as shown in Figs. 4 and 6. This indicates that the circuit has a resonance frequency with a sequence of inputs (frequency preference). This circuit also fires in response to a strong inhibitory input (amplitude: -85 nA), as shown in Fig. 7 (post-inhibitory rebound).

These results show that the RFN circuit exhibits the same behaviors as the RFN model, i.e., coincidence detection, band-pass filtering, and post-inhibitory-rebound [21].

#### 5. Conclusions

In this paper, we proposed an analog integrated circuit for implementing a resonate-and-fire neuron (RFN) model. Our circuit was designed based on the Volterra system to mimic oscillatory dynamics of the RFN model. The RFN circuit acts as a coincidence detector and a band-pass filter, and also exhibits post-inhibitory rebound. These properties are suitable for selective communication in spiking neural networks via bursts, resulting in increasing the reliability of neural information processing [22].

All MOS transistors comprising the circuit operate in their subthreshold region under low-power supply voltages. Therefore, the RFN circuit also accomplishes low-power consumption.

In conclusion, the RFN circuit is expected to be available as a building block for constructing large-

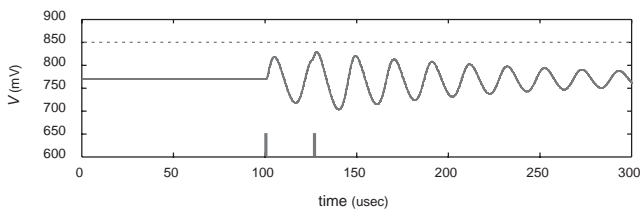


Figure 6: Non-resonant response.

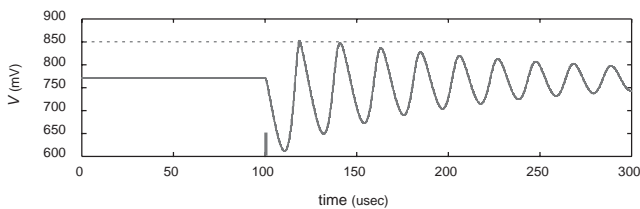


Figure 7: Post-inhibitory rebound.

scale functional spiking neural networks.

### References

- [1] C. A. Mead, *Analog VLSI and neural systems*, Addison-Wesley, Reading, 1989.
- [2] S.-C. Liu, J. Kramer, G. Indiveri, T. Delbruck, and R. Douglas, *Analog VLSI: Circuits and Principles*, MIT Press, 2002.
- [3] S.-C. Liu, J. Kramer, G. Indiveri, T. Delbruck, T. Burg, and R. J. Douglas, "Orientation-selective aVLSI spiking neurons," *Neural Networks*, vol. 14, no. 6-7, pp. 629-643, 2001.
- [4] F. Tenore, R. Etienne-Cummings, and M. A. Lewis, "A programmable array of silicon neurons for the control of legged locomotion," in *proc. IEEE Int. Symp. Circ. Syst.*, 2003.
- [5] M. Cheely and T. Horiuchi, "Analog VLSI models of range-tuned neurons in the bat echolocation system," *EURASIP J. Appl. Signal Proc.*, vol. 7, pp. 649-658, 2003.
- [6] Y. Kanazawa, T. Asai, M. Ikebe, and Y. Amemiya, "A novel CMOS circuit for depressing synapse and its application to contrast-invariant pattern classification and synchrony detection," *Int. J. Robotics and Automation*, vol. 19, no. 4, pp. 206-212, 2004.
- [7] G. Indiveri, E. Chicca and R. J. Douglas, "A VLSI array of low-power spiking neurons and bistable synapse with spike-timing dependent plasticity," *IEEE Trans. Neural Networks*, to be appeared.
- [8] R. J. Vogelstein, U. Mallik, G. Cauwenberghs, E. Culciello, and R. Etienne-Cummings, "Saliency-driven image acuity modulation on a reconfigurable silicon array of spiking neurons," *Adv. Neural Info. Proc. Syst.* vol. 16, 2005.
- [9] S. R. Schultz and M. A. Jabri, "Analogue VLSI integrate-and-fire neuron with frequency adaptation," *Electronic Letters*, vol. 31, no. 16, pp. 1357-1358, 1995.
- [10] K.A. Boahen, *Retinomorph Vision Systems: Reverse Engineering the Vertebrate Retina*, Ph.D. thesis, California Institute of Technology, Pasadena CA, 1997.
- [11] A. van Schaik, "Building blocks for electronic spiking neural networks," *Neural Networks*, vol. 14, no. 6-7, pp. 617-628, 2001.
- [12] S.-C. Liu and B. A. Minch, "Homeostasis in a silicon integrate-and-fire neuron", *Adv. Neural Info. Proc. Syst.*, vol. 13, 2001
- [13] G. Indiveri, "A low-power adaptive integrate-and-fire neuron circuit," in *proc. IEEE Int. Symp. Circ. Syst.*, 2003.
- [14] T. Asai, Y. Kanazawa, and Y. Amemiya, "A sub-threshold MOS neuron circuit based on the Volterra system," *IEEE Trans. Neural Networks*, vol. 14, no. 5, pp. 1308-1312, 2003.
- [15] H. Nakano and T. Saito, "Grouping synchronization in a pulse-coupled network of chaotic spiking oscillators," *IEEE Trans. Neural Networks*, vol. 15, no. 5, pp. 1018-1026, 2004.
- [16] E. Farquhar, P. Hasler, "A bio-physically inspired silicon neuron," *IEEE Trans. Circ. Syst. -I*, vol. 52, no. 3, pp. 477-488, 2005.
- [17] C. Rasche and R. H. R. Hahnloser, "Silicon synaptic depression," *Biol. Cybern.*, vol. 84, pp. 57-62, 2001.
- [18] S.-C. Liu, "Analog VLSI circuits for short-term dynamic synapses," *EURASIP J. Appl. Signal Proc.*, vol. 7, pp 620-628, 2003.
- [19] R. Z. Shi and T. Horiuchi, "A summing, exponentially-decaying CMOS synapse for spiking neural systems," *Adv. Neural Info. Proc. Syst.*, vol. 16, 2004
- [20] A. Bofill-i-Petit and A. F. Murray, "Synchrony detection and amplification by silicon neurons With STDP synapses, *IEEE Trans. Neural Networks*, Vol. 15, NO.5, pp. 1296- 1304, 2004.
- [21] E. M. Izhikevich, "Resonate-and-fire neurons," *Neural Networks*, vol. 14, pp. 883-894, 2001.
- [22] E. M. Izhikevich, N. S. Desai, E. C. Walcott, F. C. Hoppensteadt, "Bursts as a unit of neural information: selective communication via resonance," *Trends in Neuroscience*, vol. 26, pp. 161-167, 2003.
- [23] S. N. Goel, C. S. Maitra, and W. E. Montroll, "On the Volterra and other nonlinear models of interacting populations," *Rev. Mod. Phys.*, vol. 43, pp. 231-276, 1971.